

Fusion Hindrance in the Heavy Ion Reactions

– Border Between the Normal and Hindered Fusions

Caiwan Shen¹, David Boilley^{2,3}, Qingfeng Li¹, Junjie Shen^{1,4}, Yasuhisa Abe⁵

¹*School of Science, Huzhou Teachers College, Huzhou 313000, P.R. China*

²*GANIL, CEA/DSM-CNRS/IN2P3,*

BP 55027, F-14076 Caen cedex 5, France

³*Univ. Caen, Esplanade de la Paix,*

B.P. 5186, F-14032 Caen Cedex, France

⁴*School of Science and Information Engineering,*

Zhejiang Normal University, Jinhua 321000, P.R. China

⁵*Research Center for Nuclear Physics,*

Osaka University, Osaka 567-0047, Japan

Abstract

The fusion hindrance in heavy ion collisions is studied in the framework of the two-center liquid drop model. It appears that the neck and the radial degrees of freedom might both be hampered by an inner potential barrier on their path between the contact configuration to the compound nucleus. Heavy ion reactions with and without the two kinds of fusion hindrance are classified through systematic calculations. It is found that the number of reactions without radial fusion hindrance is much smaller than that without neck fusion hindrance, and for both kinds of fusion hindrance the number of reactions without fusion hindrance at small mass-asymmetry parameter α is smaller than that at large α . In the formation of a given compound nucleus, if a reaction with α_c is not hindered, then other reactions with $\alpha > \alpha_c$ are also not hindered as it is well known experimentally.

PACS numbers: 25.70.Gh, 25.70.Jj, 27.90.+b.

I. INTRODUCTION

The fusion hindrance that appears in heavy ion reactions has been known for many years. Now the mechanism of fusion hindrance is gradually understood as to be due to an extra internal barrier between the touching configuration and the compound shape after overcoming the Coulomb barrier [1–3]. However what causes the internal barrier is a difficult problem. One of the hypotheses is that the internal barrier could be thought as the conditional saddle point in the liquid-drop potential as well as could be attributed to an effective barrier due to the dissipation of the incident kinetic energy [4, 5].

Since there are two barriers for the fusion, its theoretical description is divided into two consecutive steps: one is from infinity to the contact configuration passing over the Coulomb barrier, and another one is from the contact point to the compound state overcoming the internal barrier. This so-called two-step model explains the extra-push energy and furthermore gives an energy dependent fusion cross sections [6, 7, 9, 10]. The measured residue cross section can be calculated by plugging a statistical evaporation model on the two-step model.

To evaluate the amplitude of the hindrance to the fusion, the size of the inner barrier is not enough. The dissipation mechanism also plays an important role and one has to solve dynamically the diffusion over this barrier. This was done analytically in one dimensional case assuming a parabolic barrier [11, 12]. Here, we will focus our attention on the appearance of the hindrance to the fusion that is due to the saddle point height measured from the energy of the touching configuration formed by the projectile and target nuclei of the incident channel. In other words, there is no hindrance for cases without internal barrier. Therefore, the border between the normal and the hindered fusion is given by the condition that the contact configuration be on the top of the saddle point.

For mass-symmetric reactions, the fusion path between the touching configuration and the compound shape can be easily determined since the system evolves only along the radial degree of freedom. In order to determine if the fusion hindrance occurred for a given reaction, we simply compare the position of the barrier and the touching configuration: the fusion exists while the barrier is located inner side of the touching point and vice versa. Ref. [13] systematically analyzed different symmetric reactions and drew a clear border between the two kinds of reactions (with and without fusion hindrance).

How is the situation for mass-asymmetric cases? Generally this problem becomes difficult because the system crosses a ridgeline, not a saddle. It is then difficult to determine an effective reaction coordinate. However there is a way to avoid the difficulty: let the reactions evolve starting from the contact point on the potential surface without any random force, and then check if the compound state is reached. If the composite system evolves toward the compound direction, it means that there is no barrier between contact point and compound state, and thus the fusion hindrance does not exist. Otherwise, the fusion hindrance occurs. With this method, the current paper studies the occurrence of the fusion hindrance for asymmetric reactions.

Refs. [16–18] show that the neck of the amalgamated system also plays an important role in the hindrance to the fusion. Thus, one of the related questions is about the evolution of neck degree of freedom: Is there also a fusion hindrance in the neck evolution, like for radial evolution?

We will answer to these questions in the present paper.

II. PARAMETERIZATION OF THE COMPOSITE SYSTEM

There are several ways to parameterize the shape of the amalgamated system. In this paper we use the so-called two-center parameterization [14, 15] based on three important parameters which are: the distance between two centers z , the mass-asymmetry parameter α , and the neck parameter ε . The dimensionless parameter z is defined as follows:

$$z = R/R_0, \quad (1)$$

where R denotes the distance between two centers of the harmonic potentials, and R_0 the radius of the spherical compound nucleus. The mass-asymmetry parameter is defined as usual,

$$\alpha = \frac{A_1 - A_2}{A_1 + A_2}, \quad (2)$$

where A_1 and A_2 are the mass numbers of the colliding nuclei. The neck parameter ε is defined by the ratio of the smoothed height at the connection point of the two harmonic potentials and that of spiked potential. In this description, nuclear shape is defined by equipotential surfaces with a constant volume. For example, $\varepsilon = 1$ means no correction, i.e., complete di-nucleus shape, while $\varepsilon = 0$ means no spike, i.e., flatly connected potential,

which describes highly deformed mono-nucleus. Thus, the neck describes shape evolution of the compound system from di-nucleus to mono-nucleus. The initial value of z , α and ε , for a given reaction at the touching point is

$$z_0 = \frac{A_p^{1/3} + A_t^{1/3}}{(A_p + A_t)^{1/3}}, \quad (3)$$

$$\alpha_0 = \frac{A_t - A_p}{A_t + A_p}, \quad (4)$$

$$\varepsilon_0 = 1, \quad (5)$$

respectively. Here A_p (A_t) stands for the mass number of the projectile (target). With this parameterization, the liquid drop model (LDM) potential is adopted to calculate the energy of the touching di-nucleus.

These three parameters are connected by the potential, the inertia and friction tensors. For the sake of comprehension, we will study the neck and the radial degrees of freedom separately.

III. FUSION HINDRANCE IN THE NECK EVOLUTION

In this section we focus our attention on the potential landscape seen by the neck parameter. Let us recall that in the two-step model, the fusion hindrance is described as the additional barrier hampering the evolution from the contact point to the compound nucleus.

In order to show the direction of evolution of the neck degree of freedom, the LDM potential is plotted as a function of ε in Fig. 1, where the different lines correspond to different distances between the projectile and target. The figure shows two different directions of evolution: (i) at small z ($z = 1.3$ or $z = 1.5$) the potential decreases with reducing neck parameter (thicker neck) which means that at contact the neck becomes thick by the driving effect of the potential. (ii) at large z ($z = 1.8$ or $z = 1.9$), the potential increases with reducing neck parameter around $\varepsilon \sim 1$ and a bump exists at a critical value of ε . This indicates that an extra energy should be provided to reach the thick neck, i.e. to form a mono-nucleus. In other words, the system is hindered to form a compound nucleus. In fact, the frontier between the two cases can be determined by the slope of the potential at the point $\varepsilon = 1$:

$$f = \left. \frac{dV}{d\varepsilon} \right|_{\varepsilon=1}. \quad (6)$$

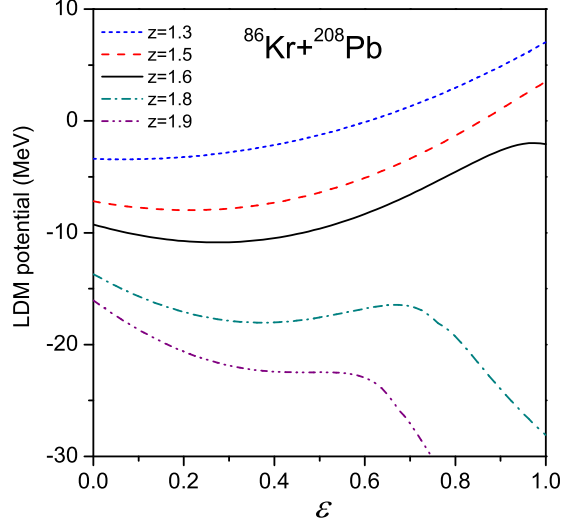


FIG. 1: LDM potential as a function of the neck parameter ε for $^{86}\text{Kr}+^{208}\text{Pb}$ at various relative distances.

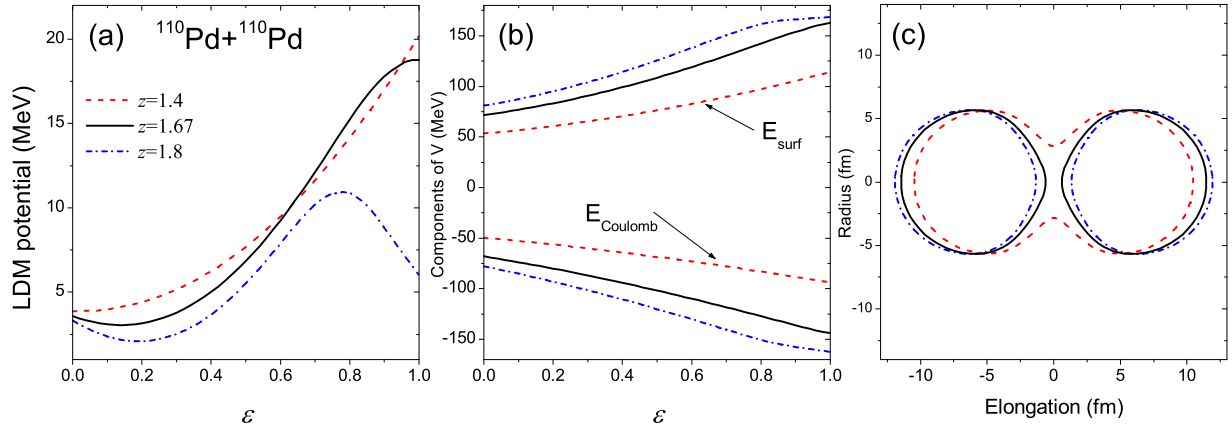


FIG. 2: LDM potential for $^{110}\text{Pd} + ^{110}\text{Pd}$. (a) LDM potential as a function of ε ; (b) Components of the LDM potential, surface potential (above zero) and Coulomb potential (below zero), as a function of ε ; (c) Di-nuclear shapes at $\varepsilon = 1$. The dashed, solid and dash-dotted lines are for $z = 1.4, 1.67, 1.8$, respectively. The slope f equals to 0 at $z = 1.67$.

Here V denotes for the LDM potential. Positive f and negative f correspond to the first case and the second case, respectively.

The reasons why the potential as a function of ε shows different features are displayed in Fig. 2. The potentials in this figure are referred to the potential at the spherical compound

state. At small relative distances z (the red dashed line), reducing ε from $\varepsilon = 1$ means decreasing the surface and thus the corresponding surface potential, while the Coulomb potential becomes larger (Fig. 2(b)). Since the surface potential reduces faster than the increasing of the Coulomb potential, the total potential becomes smaller with reducing ε , as shown by the red dashed line in Fig. 2(a). When the distance between the projectile and target increases (black solid line in Fig. 2) the decreasing speed of the surface area becomes smaller. At a critical distance z_c (for instance $z_c = 1.67$ for $^{110}\text{Pd} + ^{110}\text{Pd}$), the decreasing of the surface potential equals the increasing of the Coulomb potential with reducing ε around $\varepsilon = 1$, so that the slope at $\varepsilon = 1$ becomes zero, as shown by the solid line in Fig. 2(a)(b). While at larger z , shown by the blue dash-dotted line, the surface area is stable with reducing ε around $\varepsilon = 1$ and thus the total potential is increasing while neck starts to evolve from $\varepsilon = 1$.

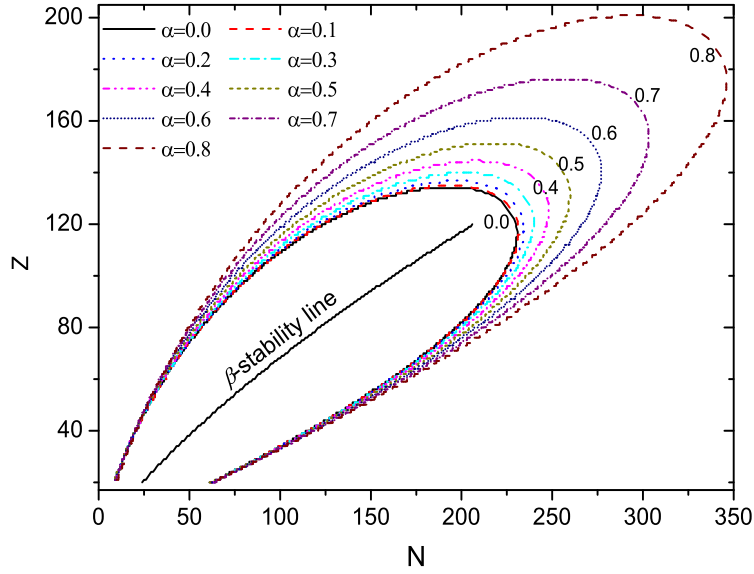


FIG. 3: The fusion reactions are classified as hindered (outside the lines) or not-hindered (inside the lines) reactions in the neck evolution. On the lines: $dV/d\varepsilon|_{(\varepsilon=1, z=z_0)} = 0$. The Z and N are the proton number and neutron number of the compound nucleus, respectively. See text for more details.

In fact we only need to know the situation at contact ($z = z_0$). By simply checking the value of f at $z = z_0$, we know whether the evolution of the neck degree of freedom is hindered or not. With this method, different combinations of the A_p and A_t for different

neutron number $N(= N_p + N_t)$ and proton number $Z(= Z_p + Z_t)$ of a compound nucleus are systematically studied and the results are shown in Fig. 3. The borderlines, corresponding to different α , are plotted connecting the reactions for which f equals 0 at $\varepsilon = 1$ and $z = z_0$. The line of β -stability is also plotted. Inside the borderlines, the slope f is greater than 0 and the reactions are not hindered, while outside the lines it is the opposite.

Comparing the area encircled with different lines, it also shows that the number of reactions without neck fusion hindrance for small α is smaller than for large α . This is due to the fact that more symmetric reactions correspond to larger Coulomb repulsion force which leads the Coulomb potential to increase more quickly with reducing ε . Since the encircled area is very large even for $\alpha = 0$, the neck evolution is not hindered for most of the realistic reactions.

IV. FUSION HINDRANCE IN THE RADIAL EVOLUTION

A. Average of the neck parameter

We have just concluded that the neck evolution is not hindered for most of the realistic reactions. In fact, once at contact a strong potential slope drives the neck degree of freedom toward a mono-nucleus shape. On the other hand, the radial and mass-asymmetry degrees of freedom face a potential barrier for systems with hindered fusion. As a consequence, the neck degree of freedom evolves faster than the other two. It has reached equilibrium before the diffusion over the potential barrier has started [16–18]. As most of the di-nucleus evolve along z and α direction with an equilibrated neck parameter, we study the fusion hindrance in the rest two degrees of freedom at the equilibrated value of ε .

The neck parameter at equilibrium can be determined through the average of ε via

$$\langle \varepsilon \rangle = \frac{\int \varepsilon w(\varepsilon) d\varepsilon}{\int w(\varepsilon) d\varepsilon}, \quad (7)$$

where $w(\varepsilon) = e^{-V(\varepsilon)/T}$, and T is the temperature of the system. As shown in Fig. 4, $\langle \varepsilon \rangle$ differs slightly for different reactions. In most cases, $\langle \varepsilon \rangle$ is close to 0.1. Therefore we take $\varepsilon = 0.1$ in the next calculations. This value is also used in the calculation of fusion cross section for ^{48}Ca induced reactions in the two-step model, and with which the residue cross sections are calculated combining the statistical evaporation model [10]. By introducing

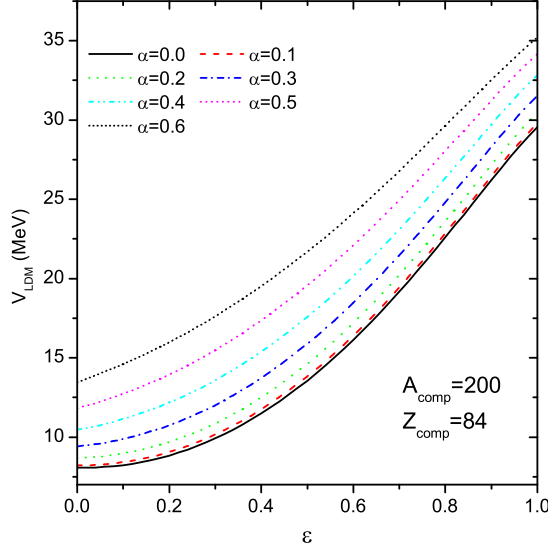


FIG. 4: LDM potential as a function of ε for different symmetric or asymmetric reactions to form ^{200}Po .

a shell energy reduction factor, the calculated residue cross sections show good agreement with experimental data from Ca + U to Ca + Bk.

B. Radial fusion hindrance

Based on the LDM, when the projectile and target evolve from the contact point to the compound state, the parameters $\{\alpha, z\}$ change from $\{\alpha_0, z_0\}$ to $\{\alpha = 0, z = 0\}$ in the same time. However because the LDM potential as a function of α at fixed z and ε is similar to a parabolic potential centered at $\alpha = 0$, the evolving system is not hindered in the mass-asymmetry direction. Therefore we only need to consider the fusion hindrance in the radial direction. Since the friction in the α and z direction is close to each other, the radial direction cannot be de-coupled from the mass-asymmetry direction. Thus in the analysis of the radial fusion hindrance we will consider α and z direction in the same footing.

It is easier to understand the radial fusion hindrance in symmetric reactions by simply comparing the contact point and the saddle point, shown in Fig. 5. In this figure ε has been fixed to 0.1. For reactions with light nuclei as $^{90}\text{Zr} + ^{90}\text{Zr}$ and $^{100}\text{Mo} + ^{100}\text{Mo}$, the saddle points are located at the right hand side of the contact line ($z_0 = 1.587$), which means that projectile and target at contact will evolve towards each other automatically by the driving

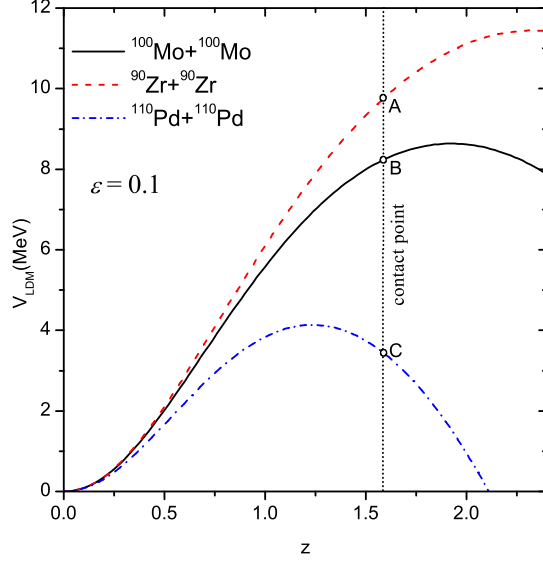


FIG. 5: The relation between the contact point and the saddle point for different reactions. The abscissa and ordinate stands for the distance between the two touching nuclei and LDM potential ($\varepsilon = 0.1$), respectively. The vertical dashed line corresponds to the contact point $z = 1.587$ for symmetric reactions.

force of the LDM potential and finally form the compound state. While for the reaction $^{110}\text{Pd} + ^{110}\text{Pd}$, it is opposite: when the two touching ^{110}Pd reach to the neck equilibrium (point “C” in Fig. 5), they need to overcome an extra-barrier to reach the compound state. In other words, the reaction is hindered, or the reaction has radial fusion hindrance. This is another fusion hindrance at the contact state besides the neck fusion hindrance.

However this method cannot be applied to asymmetric reactions because the saddle point changes into a ridgeline. But similar to the symmetric case, as we can imagine, if the contact point is located inside (left hand side of) the ridge line the reaction will reach the compound state without radial fusion hindrance, and v.v. Unfortunately, it is not easy to get the ridgeline from a potential surface. To find the fusion path by diffusion, one has to solve a Langevin equation as shown in Eq. (6) of Ref. [7]. Here, we employ another method: switching off the random force, setting the initial momentum in z and α direction as zero and then studying the evolution track of the reaction by solving the Newtonian equation. The friction tensor is calculated with the wall-and-window formula [8]. If the system reaches the compound state it means that the contact point is located inside the ridgeline, and thus

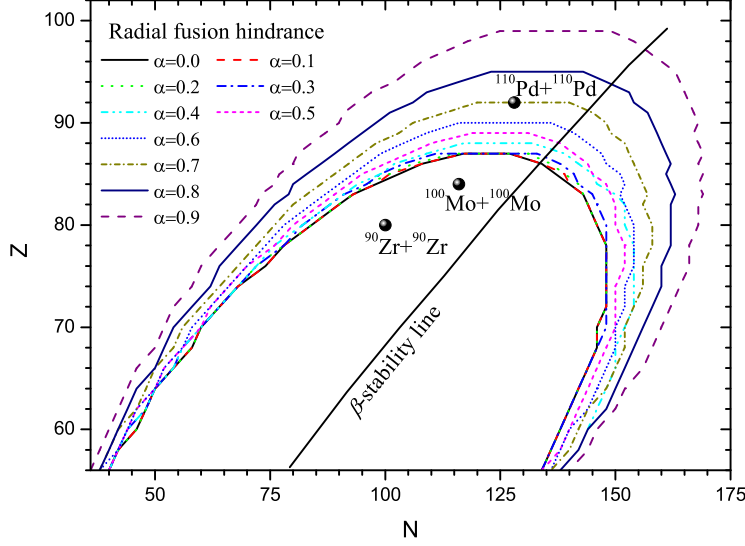


FIG. 6: Borderlines of the radial fusion hindrance. Reactions located inside the lines do not have radial fusion hindrance, while reactions located outside the lines are hindered in the radial direction. Three reactions and the line of β -stability are also plotted. The abscissa and ordinate stands for the neutron number N and proton number Z of the compound nucleus, respectively.

the system is not hindered. Contrarily the contact point is located outside the ridgeline and extra-push energy is necessary to form a compound nucleus. In fact this method can also be used for the symmetric case.

With this method we study the radial fusion hindrance in symmetric and asymmetric reactions. Fig. 6 shows the location of the borderline between hindered and non-hindered reactions for various asymmetries α . For the reactions located on the borderlines, the contact points are just located on the ridgeline, while for the reactions located inside the borderlines and outside the borderlines, the contact points are located inside and outside of the ridgeline, respectively. Therefore all of the reactions located outside of the ridgelines need extra-push energy to reach the compound state, or in other words, these reactions have radial fusion hindrance.

Fig. 6 also shows that the number of reactions without fusion hindrance at large α is larger than that at small α as it is well known experimentally. This can be easily understood: more symmetric reactions (with small α) have larger repulsive Coulomb potential ($\propto 1 - \alpha^2$) and the ridgeline is closer to or even shifted into the left side of the contact points. In the same time, with reducing α , the contact point z_0 becomes larger, as indicated in Eq. (4).

This further reduces the number of reactions without fusion hindrance at more symmetric reactions.

It is commonly known from experiment that the reactions $^{90}\text{Zr} + ^{90}\text{Zr}$, $^{100}\text{Mo} + ^{100}\text{Mo}$ are not hindered in the fusion reaction while the reaction $^{110}\text{Pd} + ^{110}\text{Pd}$ is [19–21]. The three reactions are also plotted in Fig. 6: Zr+Zr and Mo+Mo are located inside the line of $\alpha = 0$ while Pd+Pd is located outside, showing the agreement with theoretical analysis. It is interesting to see that the lower two dots (^{180}Hg : Zr+Zr and ^{200}Po : Mo+Mo) is located inside all of the lines, showing that all of the reactions to form ^{180}Hg and ^{200}Po are not hindered. While the reactions to form ^{220}U (the top dot marked by “ $^{110}\text{Pd} + ^{110}\text{Pd}$ ”) is different: because compound nucleus is located outside of the line with $\alpha < 0.7$ and inside of the line with $\alpha > 0.7$, then the reactions with $\alpha < 0.7$ are hindered while the reactions with $\alpha > 0.7$ are not.

Fig. 6 also shows that the number of reactions without fusion hindrance is limited for each asymmetric parameter α , and each line for the corresponding α has a Z_{max} . For example, $Z_{\text{max}} = 87$ for $\alpha = 0.0$ and $Z_{\text{max}} = 90$ for $\alpha = 0.6$. According to the extra-push theory[22], $Z_{\text{max}} = 86$ for $\alpha = 0$ and $Z_{\text{max}} = 110$ for $\alpha = 0.6$ if $x_{\text{th}} = 0.7$. The comparison shows that the realistic calculations give smaller Z_{max} for larger α , while for the reactions with smaller α , the two models give similar Z_{max} .

Comparing the Figs. 3 and 6, it is also found that the encircled area in Fig. 6 is much smaller than the area in Fig. 3, and the former one is completely included in the latter one. This indicates that the reactions without radial fusion hindrance are apparently without neck fusion hindrance, while the reactions with neck fusion hindrance have obviously radial fusion hindrance.

The symmetric case can be compared with the parameterized LDM proposed by Swiatecki et al.[22]. In Ref. [22], the proton number Z and the mass number A of the compound nucleus, for which the contact point of the symmetric reaction is located on the saddle point of the parameterized LDM, satisfies

$$\frac{676.48 - 38.534\sqrt{172.88 - A/2}}{5 + 1352.94/A} \leq Z \leq \frac{676.48 + 38.534\sqrt{172.88 - A/2}}{5 + 1352.94/A}. \quad (8)$$

Plotting together the above Eq. (8) and the borderline at $\alpha = 0$ of Fig. 6, we get Fig. 7. It is clear that the lower limit of N for fixed Z is almost the same between two models, but the upper limit of N is quite different: the parameterized LDM gives much larger N_{max}

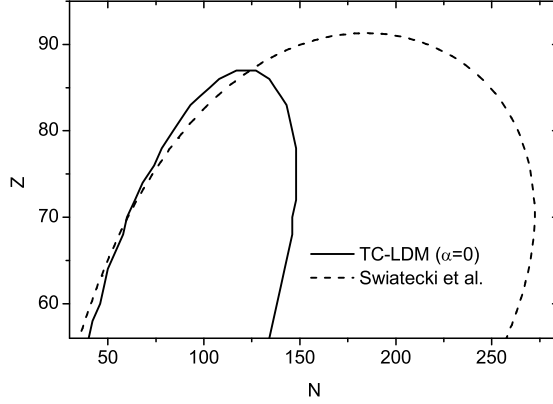


FIG. 7: Comparison of the radial fusion hindrance between the two-center LDM model (solid line) and the parameterized LDM model by Swiatecki et al. (dashed line) at $\alpha = 0$.

than the two-center LDM model. This is probably caused by the too few parameters used to describe the so complicated liquid drop energy in Ref. [22].

V. CONCLUSION

Fusion reactions between two colliding heavy ions may be hindered or not. This is explained by the appearance of an inner barrier after the contact point that hampers the formation of a compound nucleus. The liquid drop potential landscape described with the two-center parameterization for the deformation allows us to study the frontier between hindered and non-hindered reactions as shown in Fig. 3 and 6. The neck and radial degrees of freedom may both have to overcome an inner barrier to reach the compound shape. For each of them, we can draw a borderline that classifies reactions with respect to the hindrance.

It appears that for available nuclei, the neck degree of freedom is not hindered. A strong potential slope always drives it toward a mono-nucleus shape. It is not the case for the radial degree of freedom. We obtained a borderline that is far more restrictive, i.e. the hindrance to the fusion appears for compound nuclei having a charge larger than $Z = 87$ when they are formed by a symmetric reaction. The frontier is located at larger values of Z for asymmetric reactions, as it is observed experimentally.

The exact location of the border between hindered and non-hindered reactions might depend on the parameterization. It would be therefore very useful to have some experimental

results to assess the models.

Finally, it is important to note that in this paper, we have just studied the appearance of the hindrance to the fusion. The amplitude of the hindrance, i.e. the extra-energy that is necessary to the system to fuse, also depends on dynamical parameters as the friction coefficient [11, 12].

Acknowledgments

The work is supported in part by the National Natural Science Foundation of China (Nos. 10905021, 10979023, 10979024), the Key Project of the Ministry of Education of China (No. 209053), the Zhejiang Provincial Natural Science Foundation of China (No. Y6090210), and the Qian-Jiang Talents Project of Zhejiang Province (No. 2010R10102). The authors also acknowledge supports and hospitality by RCNP Osaka University, GANIL, and Huzhou Teachers College, which enable us to continue the collaboration. This work is also partly supported by the C3S2 computing center in Huzhou Teachers College.

-
- [1] S. Bjornholm, W. J. Swiatecki, Nucl. Phys. A391, 471 (1982).
 - [2] G. Royer, B. Remaud, Nucl. Phys. A444, 477(1985).
 - [3] J. P. Blocki, H. Feldmeier, W. J. Swiatecki, Nucl. Phys. A459, 145(1986).
 - [4] D. H. E. Gross, H. Kalinowski, Phys. Rep. 45, 175 (1978).
 - [5] P. Fröbrich, Phys. Rep. 116, 337 (1984).
 - [6] Y. Abe, Eur. Phys. J. A 13, 143 (2002).
 - [7] C. W. Shen, G. Kosenko, Y. Abe, Phys. Rev. C 66, 061602 (2002).
 - [8] J. Blocki et al., Ann. Phys. (N.Y.) 113, 330 (1978).
 - [9] Y. Abe, D. Boilley, G. Kosenko, Prog. Theor. Phys. Suppl. 146, 104 (2002).
 - [10] C. W. Shen, Y. Abe, D. Boilley, G. Kosenko, E. G. Zhao, Int. J. of Mod. Phys. E 17 (supp), 66 (2008).
 - [11] Y. Abe, D. Boilley, B. G. Giraud, T. Wada, Phys. Rev. E 61, 1125 (2000).
 - [12] D. Boilley, Y. Abe and J.D. Bao, Eur. Phys. J. A18, 627 (2003)
 - [13] C. W. Shen, Y. Abe, Q. F. Li, D. Boilley, Sci. China Ser. G 52, 1458 (2009).

- [14] K. Sato, A. Iwamoto, K. Harada, S. Yamaji and S. Yoshida, Z. Phys. A288, 383 (1978).
- [15] J. Maruhn and W. Greiner, Phys. Rev. Lett. 32, 548 (1974).
- [16] Y. Abe, C.W. Shen, G. Kosenko, D. Boilley and B. Giraud, Int. J. Mod. Phys. E17, 2214 (2008).
- [17] D. Boilley, Y. Abe, C.W. Shen and B. Yilmaz, CERNProceedings-2010-001, 479 (2010).
- [18] D. Boilley, C. W. Shen, Y. Abe, B. G. Giraud, in preparation.
- [19] J. G. Keller, K.-H. Schmidt, F. Hessberger, et al., Nucl. Phys. A 452, 173 (1986).
- [20] K.-H. Schmidt and W. Morawek, Rep. Prog. Phys. 54, 949 (1991).
- [21] W. Morawek, D. Ackermann, T. Brohm, et. al., Z. Phys. A 341, 75 (1991).
- [22] W. J. Swiatecki, K. Siwek-Wilczyńska, and J. Wilczyński, Phys. Rev. C 71, 014602 (2005).